Biochemistry

Article

pubs.acs.org/biochemistry

Biochemical Characterization of the Functional Roles of Residues in the Active Site of the β-Galactosidase from *Bacillus circulans* ATCC 31382

Huifang Yin,[†] Tjaard Pijning,[‡] Xiangfeng Meng,[†] Lubbert Dijkhuizen,*[,†] and Sander S. van Leeuwen[†]

[†]Microbial Physiology, Groningen Biomolecular Sciences and Biotechnology Institute (GBB), University of Groningen, Nijenborgh 7, 9747 AG Groningen, The Netherlands

[‡]Biophysical Chemistry, Groningen Biomolecular Sciences and Biotechnology Institute (GBB), University of Groningen, Nijenborgh 7, 9747 AG Groningen, The Netherlands

Supporting Information

ABSTRACT: The β-galactosidase enzyme from *Bacillus circulans* ATCC 31382 BgaD is widely used in the food industry to produce prebiotic galactooligosaccharides (GOS). Recently, the crystal structure of a C-terminally truncated version of the enzyme (BgaD-D) has been elucidated. The roles of active site amino acid residues in β-galactosidase enzyme reaction and product specificity have remained unknown. On the basis of a structural alignment of the β-galactosidase enzymes BgaD-D from *B. circulans* and BgaA from *Streptococcus pneumoniae*, and the complex of BgaA with LacNAc, we identified eight active site amino acid residues (Arg185, Asp481, Lys487, Tyr511, Trp570, Trp593, Glu601, and Phe616) in BgaD-D. This study reports an investigation of the functional roles of these residues, using site-directed mutagenesis, and a detailed biochemical characterization and product profile analysis of the mutants obtained. The data show that these residues are involved in binding and positioning of the substrate and thus determine the BgaD-D activity and product linkage specificity. This study provides detailed insights into the structure−function relationships of the *B. circulans* BgaD-D enzyme, especially regarding GOS product linkage specificity, allowing the rational mutation of β-galactosidase enzymes to produce specific mixtures of GOS structures.

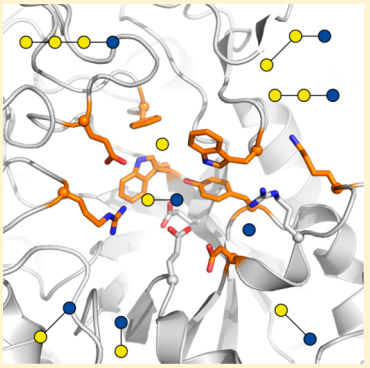

Prebiotics were first defined as "nondigestible food ingredients that beneficially affect the host by selectively stimulating the growth and/or activity of one or a limited number of bacterial species already resident in the colon, and thus attempt to improve host health".[1] This concept has been updated and adapted many times,[2−4] but there is no doubt that galactooligosaccharides (GOS) make up an important category of prebiotics. GOS are a mixture of oligosaccharides produced from lactose by β-galactosidase enzymes, comprising a number of galactose units, with a terminal glucose or galactose.[5−7] They are produced via the double-displacement reaction catalyzed by β-galactosidase enzymes. In the first step, the glycosidic linkage of lactose is cleaved, and the galactosyl unit covalently binds to the enzyme forming a galactosyl−enzyme intermediate while releasing the glucose. In the second step, an acceptor substrate attacks the intermediate, resulting in formation of a product with the galactosyl moiety. β-Galactosidase enzymes perform two reactions depending on the acceptor substrate. With water serving as the acceptor substrate, galactose is released via hydrolysis; with lactose or other carbohydrates serving as acceptor substrates, GOS products are formed via transgalactosylation.[8−11]

β-Galactosidase enzymes belong to glycoside hydrolase (GH) families 1, 2, 35, and 42.[12] The β-galactosidase from *Bacillus circulans* ATCC 31382 (BgaD, GH2) is a 189 kDa enzyme, and its commercial preparation, Biolacta N5, is widely used in the food industry.[13−15] BgaD has an activity toward lactose higher than those of and a thermal stability better than those of other β-galactosidase enzymes.[16] A study investigated the influence of organic solvents on the regioselectivity of BgaD transglycosylation.[17] The product specificity of BgaD with lactose as a substrate was studied using methylation analysis, mass spectrometry (MS), and nuclear magnetic resonance spectroscopy; in this way, 11 GOS structures were identified.[18] A detailed analysis of the commercial product Vivinal GOS, synthesized by the *B. circulans* enzyme, resulted in identification of a total of 43 GOS structures.[6,7] In *B. circulans*, BgaD is present in different isoforms resulting from C-terminal cleavage by an endogenous protease.[19] Three isoforms were reported by Vetere and Paoletti;[20] four isoforms (BgaD-A, BgaD-B, BgaD-C, and BgaD-D) were reported in the commercial enzyme preparation of β-galactosidase from *B. circulans*.[19] In recent years, these BgaD isoforms have been characterized in more detail, facilitated by their cloning and recombinant overexpression in *Escherichia coli*.[21] All four isoforms have similar

Received: March 7, 2017
Revised: May 14, 2017
Published: May 24, 2017

DOI: 10.1021/acs.biochem.7b00207
Biochemistry 2017, 56, 3109−3118

transgalactosylation activity at high lactose concentrations.[9,22] The products synthesized by recombinant BgaD-D were also studied in detail, showing a product profile similar to that of Vivinal GOS.[6,7,10] Mutagenesis studies have shown that the C-terminal discoidin domain of BgaD is essential for the hydrolytic activity of the enzyme.[23] A few BgaD-D mutants have been biochemically characterized in our previous work, resulting in identification of residues Glu532 and Glu447 as the nucleophile and acid/base catalysts, respectively.[9] Mutagenesis of the Arg484 changed the GOS linkage specificity.[11]

The high-resolution crystal structure of the shortest isoform of β-galactosidase from *B. circulans* [BgaD-D, Protein Data Bank (PDB) code 4YPJ] was reported recently.[24] Details of the structure−function relationships of this enzyme determining its GOS product linkage specificity have remained unknown. Here we report the identification and site-directed mutagenesis of further residues in the active site of BgaD-D. Their functional roles were characterized by analyzing the biochemical properties of the mutant enzymes and the structures of the GOS produced. The data provide insight into how these residues contribute to determining enzyme activity and GOS linkage specificity.

EXPERIMENTAL PROCEDURES

Bacterial Strains. *E. coli* DH5α (Phabagen) was used for DNA manipulation, and *E. coli* BL21 (DE3) was used for protein expression.

Sequence and Structure Alignment. T-Coffee and Jalview were used for the alignment of the amino acid sequences of β-galactosidases from GH2 (Table 1 and Figure 1):

Table 1. Comparison of the Amino Acid Sequences of β-Galactosidase BgaD-D from *B. circulans* ATCC 31382 and Other β-Galactosidases in the GH2 Family

enzyme name	enzyme source	identity (%)	UniProt code	PDB code
BgaD-D	*B. circulans* ATCC 31382	100	E5RWQ2	4YPJ
BgaA	*S. pneumoniae* serotype 4	49	A0A0H2UP19	4CU6
BIF3	*Bi. bifidum* DSM 20215	44	Q9F4D5	
BbgIII	*Bi. bifidum* NCIMB 41171	43	A4K5H9	
BbgIII	*Bi. bifidum*	26	D4QAP3	5DMY

BgaD-D (E5RWQ2) from *B. circulans* ATCC 31382, BgaA (A0A0H2UP19) from *Streptococcus pneumoniae* serotype 4, BIF3 (Q9F4D5) from *Bifidobacterium bifidum* DSM 20215, BbgIII (A4K5H9) from *Bi. bifidum* NCIMB 41171, and BbgIII (D4QAP3) from *Bi. bifidum*. PyMOL (The PyMOL Molecular Graphics System, version 1.2, Schrödinger, LLC) was used for the structural alignment (Figure 2) of BgaD-D from *B. circulans* (PDB code 4YPJ) and the nucleophile mutant (E645Q) of BgaA in complex with *N*-acetyl-lactosamine (LacNAc) from *S. pneumoniae* (PDB code 4CUC).

Site-Directed Mutagenesis. Plasmid pET-15b-LIC containing the rBgaD-D-encoding gene from *B. circulans* was obtained from a previous study and used as a template for site-directed mutagenesis.[10] On the basis of the results of the sequence and structure alignments, mutations of residues Arg185, Asp481, Lys487, Tyr511, Trp570, Trp593, Glu601, and Phe616 were introduced by various primers (Table S1) using the QuikChange site-directed mutagenesis kit (Stratagene). The polymerase chain reaction (PCR) products were cleaned up with a PCR purification kit after digestion by DpnI (Thermo Fisher). Then the PCR products were transformed into *E. coli* DH5α competent cells (Phabagen) via heat shock for overnight growth on LB agar plates (containing 100 μg/mL ampicillin). For every mutant, colonies were randomly chosen and inoculated into 5 mL of LB medium (containing 100 μg/mL ampicillin) for DNA amplification overnight. The plasmid DNA of the overnight cultures was purified using a miniprep kit (Sigma-Aldrich) and sequenced (GATC Biotech).

Recombinant Protein Expression and Purification. The sequence-verified plasmids were transformed into *E. coli* BL21 (DE3) (Invitrogen) competent cells for protein expression as described previously.[10] Briefly, after growth on LB agar plates (containing 100 μg/mL ampicillin), colonies were inoculated into 10 mL of LB medium (containing 100 μg/mL ampicillin) for overnight preculture. The overnight cultures were inoculated into 1 L of LB medium (containing 100 μg/mL ampicillin) and incubated at 37 °C until the cell density reached 0.6 at 600 nm; then 1 mM isopropyl β-D-thiogalactopyranoside was used for the induction of recombinant protein expression. The cells were cultured at 30 °C overnight and harvested by centrifugation at 10876*g* for 15 min. The cell pellets were washed with 20 mM Tris-HCl buffer (pH 8.0) and centrifuged again.

The cell pellets were lysed with B-PER protein extract reagent (Thermo Scientific) at room temperature for 1 h. The cell debris was removed by centrifugation; the remaining supernatants were mixed with HIS-Select Nickel Affinity Gel (Sigma) and incubated at 4 °C overnight. Unbound proteins were washed away with 20 mM Tris-HCl (pH 8.0) and 50 mM NaCl. The recombinant proteins were eluted with 20 mM Tris-HCl (pH 8.0) and 50 mM NaCl containing 100 mM imidazole. Subsequently, the imidazole was removed by ultrafiltration (30 kDa cutoff, Amicon, Merck)

Enzyme Activity Assay. For the activity assay of the wild-type and mutant enzymes, 0.5−1 mg/mL (protein concentration determined by a Nanodrop 2000 UV−vis spectrophotometer) amounts were incubated with 10% (w/w) lactose in 100 mM sodium phosphate buffer (pH 6.0) for 5 min at 40 °C. The incubation mixtures were withdrawn and immediately inactivated with 50 μL of 1.5 M NaOH. The reaction mixtures were neutralized with 50 μL of 1.5 M HCl after 10 min. The total activity (units) toward lactose was defined as the amount of enzyme required to release 1 μmol of Glc/min. The released glucose was measured using a GOPOD kit (D-glucose Assay Kit, Megazyme). The activity of the wild-type enzyme was regarded as 100%; activities of all mutant enzymes were relative to that of the wild-type enzyme. The kinetic parameters (K_m and k_{cat}) of mutant enzymes were determined using 10 different lactose concentrations ranging from 10 to 500 mM.

GOS Production and Analysis. GOS were produced by using 3.75 units/g lactose β-galactosidase wild-type and mutant enzymes with 50% (w/w) lactose [in 100 mM sodium phosphate buffer (pH 6.0)] incubated at 60 °C for 20 h to reach the highest GOS yield. We stopped the reactions by heating the mixtures at 100 °C for 10 min.

The reaction mixtures were diluted 1000-fold with Milli-Q water and analyzed by high-pH anion exchange chromatography (HPAEC) coupled with a pulsed amperometric detector (PAD) on an ICS3000 chromatography workstation (Thermo-Scientific). The analysis was performed by injecting 5 μL on a

DOI: 10.1021/acs.biochem.7b00207
Biochemistry 2017, 56, 3109−3118

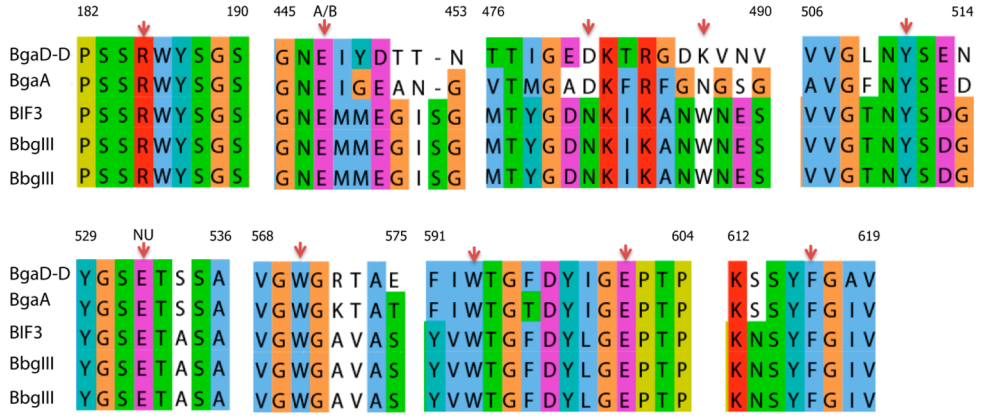

Figure 1. Sequence alignment of β-galactosidase enzymes in the GH2 family. Residues selected for mutagenesis and the catalytic residues in BgaD-D from *B. circulans* ATCC 31382, Arg185, Glu447 (acid/base catalyst), Asp481, Lys487, Tyr511, Glu532 (nucleophile), Trp570, Trp593, Glu601, and Phe616, are denoted with red arrows. The order of the sequences shown is the same as those listed in Table 1. The amino acid residue color coding used is in Clustal X format. For details, see http://www.jalview.org/help/html/colourSchemes/clustal.html; gaps in the alignments are denoted with hyphens.

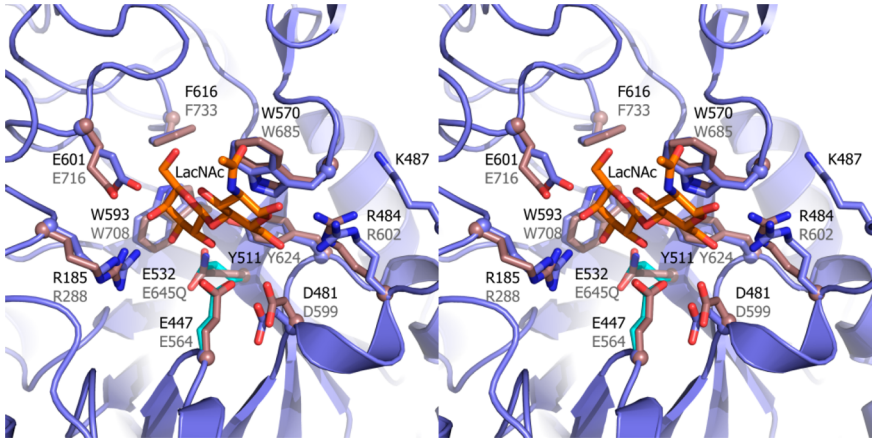

Figure 2. Stereoview of the superposition of the active sites of the β-galactosidases BgaD-D (PDB code 4YPJ) of *B. circulans* ATCC 31382 and the nucleophile mutant E645Q of BgaA from *S. pneumoniae* in complex with LacNAc (PDB code 4CUC). 4YPJ is colored slate blue and 4CUC brown, and the catalytic residues of BgaD-D are colored cyan. Residues of BgaD-D are labeled in black and the corresponding residues in BgaA in gray.

CarboPac PA1 analytical column (2 mm × 250 mm) with the following elution buffers: (A) 100 mM sodium hydroxide, (B) 600 mM sodium acetate in 100 mM sodium hydroxide, (C) Milli-Q water, and (D) 50 mM sodium acetate. The separation conditions were the same as used in our previous study.[10] The quantity of β-D-Gal*p*-(1→3)-β-D-Gal*p*-(1→4)-D-Glc*p* was determined by using a calibration curve of this compound (Sigma) ranging from 4 to 200 μg/mL. The comparisons of other GOS fractions were based on the peak intensities of HPAEC−PAD profiles of the wild-type and mutant enzymes. The quantification of the GOS yield {GOS yield (grams) = initial lactose (grams) − [remaining lactose (grams) + galactose (grams) + glucose (grams)] after 20 h} was based on a calibration curve of galactose, glucose, and lactose ranging from 10 to 1000 μM.

RESULTS

Structural Alignment. The β-galactosidase proteins BgaD-D of *B. circulans* and BgaA of *S. pneumonia* share 49% sequence identity. A structural alignment of BgaD-D (PDB code 4YPJ) with the catalytic region of BgaA (PDB code 4CU6) and with the inactive BgaA mutant E645Q in complex with LacNAc (PDB code 4CUC) (Figure 2) guided our selection of active site residues to be mutated. The residues targeted for mutagenesis were grouped in four sets, mainly based on their location in the active site.

Site-Directed Mutagenesis and Enzyme Activity. Mutations were introduced by site-directed random mutagenesis as described in Experimental Procedures. The mutants were obtained via two rounds of mutagenesis. Universal primer pairs (Table S1) were used for the first round, and 20 colonies were selected randomly for sequencing. Specific primers (Table S1) were used in the second round of mutagenesis for a full coverage of amino acid (side chain) classes, or to obtain a specific amino acid residue. The mutants obtained in the two mutagenesis rounds and their relative enzyme activities (release of Glc from lactose) are listed in Table 2. For residues Arg185, Glu601, and Tyr511, a total of 6, 11, and 5 different mutants were obtained after two rounds, respectively; all mutants were completely inactive (Table 2). Four Trp570 mutants were found in the first round of mutagenesis; another six mutants were selected in the second round. Of these mutants, Trp570Tyr had the highest activity, 37.4 ± 0.4% compared to that of the wild-type enzyme, followed by Trp570Phe (16.1 ± 1.0%) and Trp570Leu (14.6 ± 0.8%). The activity of the other Trp570 mutants was rather low (Table 2).

DOI: 10.1021/acs.biochem.7b00207
Biochemistry 2017, 56, 3109−3118

Table 2. Relative Total Activities (release of Glc from lactose) of the Various *B. circulans* ATCC 31382 β-Galactosidase BgaD-D Mutant Proteins

site	round	mutant	relative activity[a]	site	round	mutant	relative activity
		WT	100	Phe616	1	Val	1.9 ± 0.01
Arg185	1	Glu	*b*			Glu	1.4 ± 0.01
		Gly	*b*			Gly	3 ± 0.1
		Leu	*b*			Lys	0.8 ± 0.01
		Pro	*b*			Gln	3.2 ± 0.08
		Ser	*b*			Arg	1.3 ± 0.01
		Lys	*b*			Asp	4.6 ± 0.1
Glu601	1	Pro	*b*			Leu	22.9 ± 1.6
		Phe	*b*		2	Trp	37.2 ± 1.5
		Gln	*b*			His	13.4 ± 0.2
		His	*b*			Ser	5.3 ± 1.1
		Ala	*b*			Thr	4.9 ± 0.03
		Arg	*b*			Asn	11.6 ± 0.1
		Tyr	*b*			Cys	3.9 ± 0.08
		Cys	*b*			Pro	3.8 ± 0.7
		Gly	*b*			Ala	3.4 ± 0.1
		Thr	*b*			Ile	2.8 ± 0.04
	2	Asp	*b*			Met	1.4 ± 0.05
Tyr511	1	Cys	*b*			Tyr	73.2 ± 0.6
		Pro	*b*	Asp481	1	Tyr	*b*
		Ser	*b*			Phe	*b*
	2	Trp	*b*			Glu	7.3 ± 0.5
		Phe	*b*			His	2.1 ± 0.6
Trp570	1	Gly	5.1 ± 0.08			Ala	*b*
		Thr	6.5 ± 0.2			Ser	6.1 ± 0.2
		Arg	3.6 ± 0.1		2	Lys	*b*
		Glu	5.2 ± 0.3			Arg	*b*
	2	Tyr	37.4 ± 0.4			Asn	6.7 ± 0.3
		Phe	16.1 ± 1.0			Gln	3.3 ± 0.3
		Ala	4.2 ± 0.05			Leu	*b*
		Val	3.0 ± 0.1			Trp	*b*
		Cys	6.1 ± 0.1			Gly	*b*
		Leu	14.6 ± 0.8	Lys487	1	Met	105.5 ± 1.2
Trp593	1	Val	*b*			Phe	73.2 ± 0.7
		Leu	*b*			Leu	93.7 ± 0.4
		Ser	*b*			Gln	83.1 ± 0.6
		Ala	*b*			Ser	76.3 ± 0.9
		Gly	*b*			Gly	65.5 ± 0.9
		Thr	*b*			Asn	65.5 ± 0.8
		Pro	*b*			Cys	3.5 ± 0.4
		Gln	*b*				
		Tyr	3.3 ± 0.2				
		Phe	70.7 ± 0.7				
		His	*b*				

[a]Total activity. Activities of all mutant enzymes are relative to that of the wild-type (WT) enzyme (100%, 103.4 μmol min^{-1} mg^{-1}). Enzyme activity was measured in triplicate experiments with 10% (w/w) lactose at 40 °C. [b]Activity not detectable (detection limit of 0.1 mg/mL glucose).

One round of Trp593 mutagenesis yielded a total of 11 mutants. Among them, only Trp593Tyr and Trp593Phe retained activity, 3.3 ± 0.2 and 70.7 ± 0.7% of the wild-type enzyme activity, respectively (Table 2). For Phe616, a total of eight mutants were obtained in the first round. With the specific primers, the other 11 mutants were also obtained. Phe616Trp (37.2 ± 1.5%) and Phe616Tyr (73.2 ± 0.6%) had the highest activity among all these mutants (Table 2). In the first round, six mutants of Asp481 were acquired, and another seven mutants were obtained in the second round. Only Asp481Glu, Asp481His, Asp481Ser, Asp481Asn, and Asp481Gln retained very little activity (Table 2). For Lys487, the universal primers resulted in eight mutants; most of them had relatively high activity (65.5 ± 0.8 to 105.5 ± 1.2%), except for Lys487Cys (3.5 ± 0.4%) (Table 2).

Catalytic Properties. On the basis of the activity compared to that of the wild-type (WT) enzyme, and interesting product profiles (see the next section), the catalytic properties of a selection of enzymes were determined (Table 3). For all enzymes, the k_{cat} was lower (12.3 ± 1.1 to 184.7 ± 3.4 s^{-1}) than that of the WT enzyme (199.8 ± 5.3 s^{-1}), while the substrate affinity (K_m) ranged from 21.9 ± 4.7 to 246.5 ± 66.0 mM; the WT enzyme has a K_m of 112.9 ± 12.7 mM.[11] The catalytic efficiency (k_{cat}/K_m) of the WT enzyme is 1780.7 ± 152.0 s^{-1} M^{-1};

DOI: 10.1021/acs.biochem.7b00207
Biochemistry 2017, 56, 3109−3118

Table 3. Kinetic Properties of the *B. circulans* ATCC 31382 Wild-Type β-Galactosidase BgaD-D and Mutant Proteins

enzyme	K_m[a] (mM)	k_{cat}[a] (s^{-1})	k_{cat}/K_m (s^{-1} M^{-1})
WT[b]	112.9 ± 12.7	199.8 ± 5.3	1780.7 ± 152.0
Trp570Tyr	75.6 ± 11.0	27.2 ± 0.9	398.6 ± 20.0
Trp570Phe	246.5 ± 66.0	44.6 ± 7.1	178.4 ± 16.5
Trp593Phe	21.9 ± 4.7	63.6 ± 0.6	2990.2 ± 184.2
Phe616Trp	180.0 ± 8.0	114.7 ± 3.5	587.7 ± 5.2
Phe616His	156.1 ± 9.8	48.9 ± 1.8	321.3 ± 27.2
Phe616Tyr	112.6 ± 3.9	183.9 ± 4.0	1504.6 ± 57.2
Asp481Gln	57.4 ± 13.8	12.3 ± 1.1	217.9 ± 37.9
Lys487Ser	119.5 ± 5.6	184.7 ± 3.4	1546.3 ± 50.0
Lys487Gly	176.8 ± 12.6	177.7 ± 7.1	1001.5 ± 37.2

[a]Kinetic parameters (K_m and k_{cat}) were determined with 10 different lactose concentrations ranging from 10 to 500 mM. [b]Data from our previous study.[11]

in almost all mutants, the efficiency was lower (178.4 ± 16.5 to 1546.3 ± 50.0 s^{-1} M^{-1}), except for Trp593Phe that has a much higher k_{cat}/K_m of 2990.2 ± 184.2 s^{-1} M^{-1}.

Mutant GOS Profiles. For the wild type (WT) and a selection of mutant enzymes showing sufficient activity, incubations using 3.75 units/g of lactose were performed for 20 h, and the HPAEC−PAD GOS product profiles were compared (Figure 3).

Because galactose is released by hydrolysis, the hydrolysis activity is reflected by the intensity of peak **1** (galactose). For all three Trp570 mutants, the hydrolysis activity increased, as evidenced by the increased intensity of peak **1** in the HPAEC−PAD profile (Figure 3A), whereas the hydrolytic activity of all Trp593 and Phe616 mutant enzymes was comparable with that of the WT enzyme [peak **1** (Figure 3B,C)]. Most notable changes in relative product intensities were observed in structures **8**, **11**, **13**, and **17** for the mutant enzymes at Trp570, Trp593, and Phe616 (Table 4). In the case of Trp570Tyr and Trp570Phe, structures **8a** [β-D-Gal*p*-(1→2)-D-Glc*p*] and **8b** [β-D-Gal*p*-(1→3)-D-Glc*p*] were similar in level to that of the WT enzyme, whereas the levels of the (β1→4) elongations (peaks **13a** and **13b**) significantly increased. Levels of structures **11** [β-D-Gal*p*-(1→4)-β-D-Gal*p*-(1→4)-D-Glc*p*] and its (β1→4) elongation (peak **17**) were significantly decreased. In the case of Trp593Tyr and Trp593Phe, a similar observation was made, except that levels of structures **8a** and **8b** also were increased compared to the WT product profile. Mutant Trp570Leu showed a completely different profile, with a hydrolytic activity much higher than those of any of the other mutants. The HPAEC−PAD profile showed two major product peaks for **11** and **17** and only minor peaks for other products. However, quantitation of the peaks (Table 4) showed that peak **11** is comparable with that of the WT enzyme, while all other peaks showed a reduced product yield.

Enzymes with a mutation at Phe616 showed HPAEC−PAD profiles very similar to that of the WT enzyme. Quantitation of peaks **8**, **11**, **13**, and **17** showed some differences in intensity compared with the WT enzyme, but the changes were mostly minor. In case of Phe616 Trp, -Asn, and -Tyr mutants, levels of structures **11** and **17** were slightly increased, while levels of **8** and **13** were either slightly decreased or the same compared to that of the WT. For the other Phe616 mutants, the intensities showed the opposite response (Table 4).

Mutations at Asp481 and Lys487 showed different effects on the product profiles (Figure 3D,E). Mutation of Asp481 to Glu, Ser, or Asn reduced the intensity of peaks **8**, **11**, and **13** (Table 5), whereas the intensity of peak **12** [β-D-Gal*p*-(1→3)-β-D-Gal*p*-(1→4)-D-Glc*p*] increased significantly. Whereas the WT enzyme produces only minor amounts of **12** (0.2 ± 0.05 g/100 g of lactose), all three mutants produced a significant amount of **12**. Notably, in case of Asp481Asn, the intensity of peak **4** [β-D-Gal*p*-(1→4)-D-Glc*p*] also was increased (Figure 3D).

Changing Lys487 to a Met, Leu, or Gln had no significant effect on the product profile, also evidenced by quantitation of peaks **8** and **11**−**13** (Table 5). Mutation of this residue to Phe or Asn resulted in a reduced yield for **8** and **13**, while the yields of **11** and **12** both increased. The most remarkable changes were observed for mutants Ly487Ser and Lys487Gly, showing a significant increase in **12**, even up to 9.7 ± 1.1 g/100 g of lactose.

DISCUSSION

Prebiotic GOS produced from lactose by β-galactosidase enzymes are drawing a great deal of attention; they have been added to infant formula because their molecular size is similar to that of human milk oligosaccharides and because of their beneficial functions and positive effects on intestinal health.[25−28] The beneficial functions of GOS were further shown by studies regarding calcium absorption, metabolic activities, and protection against colorectal cancer.[29−32] To understand how different β-galactosidases synthesize such a range of GOS structures, and how they may be tailored to produce more specific GOS mixtures, it is essential to obtain detailed (three-dimensional) structural information about both the enzymes and their GOS products. Although several crystal structures of β-galactosidase enzymes have been determined and served to improve our understanding of the enzyme reaction mechanism,[33−36] their detailed structure−function relationships are still largely unexplored, especially regarding their GOS product linkage specificity.

In this study, we have characterized the functional roles of eight amino acid residues in the active site of BgaD-D from *B. circulans* ATCC 31382, close to the substrate binding site, constituting four groups.

Arg185 and Glu601 Are Essential for Activity and Substrate Binding. Arg185 and Glu601 are located near the nonreducing end hydroxyl groups of the lactosyl moiety of LacNAc in subsite −1 (Figure 4A). All six mutants of Arg185, and all 11 mutants of Glu601, had lost detectable enzyme activity. As shown in Figure 4A, Arg185 and Glu601 in 4YPJ correspond to Arg288 and Glu716 in *S. pneumoniae* BgaA, respectively; they are located at the −1 subsite of BgaA and are hydrogen-bonded to the 4-OH group of the galactosyl unit of LacNAc (Figure 4A). Given the conservation of these residues, it is likely that Arg185 and Glu601 in BgaD-D have a similar essential function, namely assisting in the binding and positioning of the substrate.

Tyr511 Is Essential for Activity. Residue Tyr511 is conserved among the GH2 family β-galactosidase enzymes (Figure 1); both in BgaA and in BgaD, its OH group makes a hydrogen bond interaction (2.6 Å) to the nucleophilic Glu residue. The nearby nucleophilic residue Glu532 attacks the substrate while it is productively bound; a previous study proposed that Tyr511 assists in the catalytic mechanism by donating its proton to Glu532, before it attacks the substrate to form the covalent galactosyl−enzyme intermediate.[24] None of the mutants obtained were active. Our experimental results

DOI: 10.1021/acs.biochem.7b00207
Biochemistry 2017, 56, 3109−3118

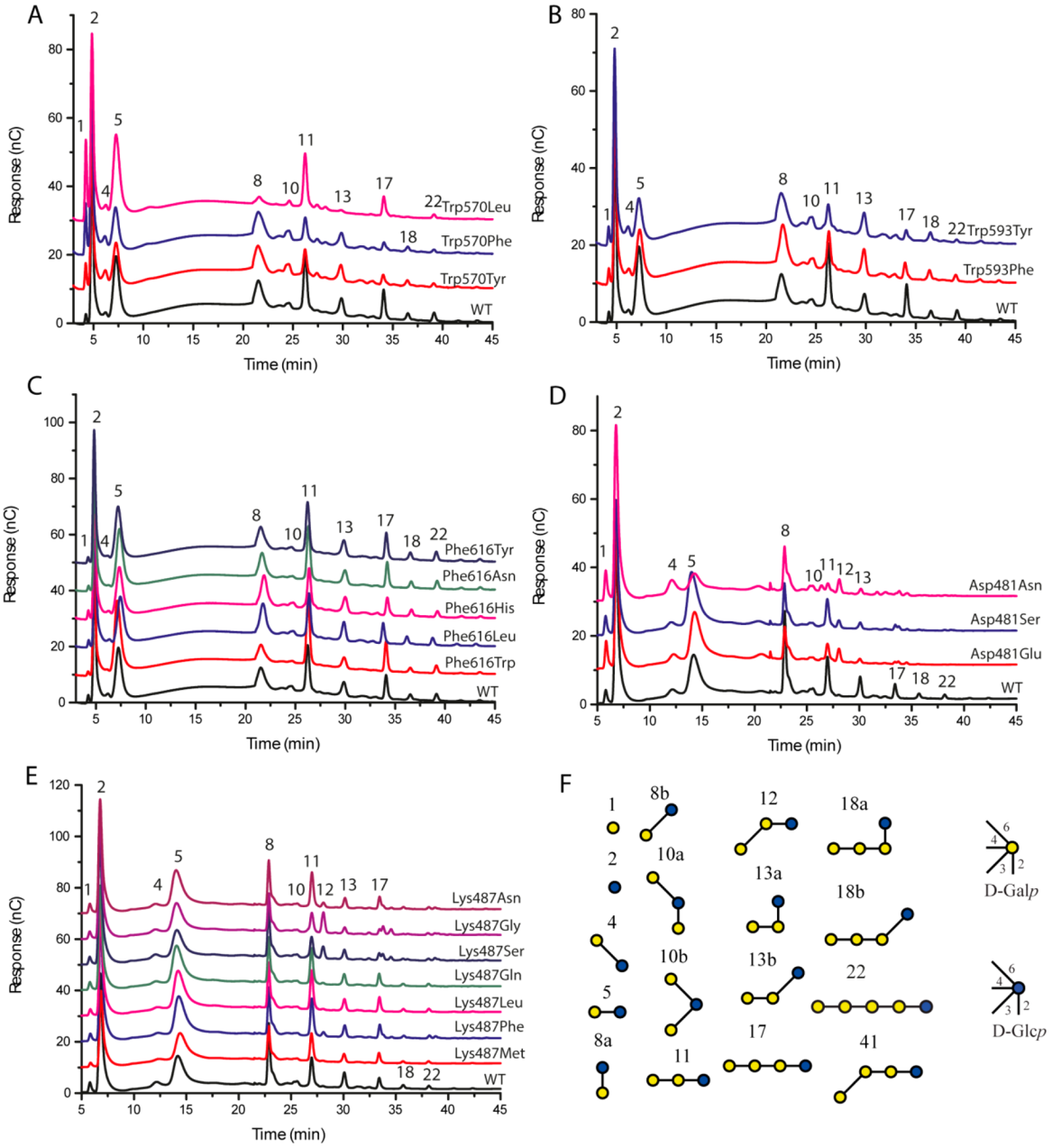

Figure 3. HPAEC−PAD analysis of the GOS profiles produced by *B. circulans* ATCC 31382 BgaD-D WT and mutant enzymes: (A) Trp570 mutants, (B) Trp593 mutants, (C) Phe616 mutants, (D) Asp481 mutants, (E) Lys487 mutants, and (F) the annotated major GOS structures. WT and mutant enzymes (3.75 units/g of lactose) were incubated with 50% (w/w) lactose (structure **5**) for 20 h at 60 °C.

confirm that the hydroxyl group of Tyr511 is essential for enzymatic activity.

Residues Trp570, Trp593, and Phe616 Form an Aromatic Pocket Shaping the Substrate Binding Site. Trp570 is located near the +1 subsite, while Trp593 and Phe616 are located near the −1 subsite (Figure 4B). From the 10 mutants of Trp570, Trp570Tyr retained 37.4 ± 0.4% of the WT activity (Table 2). The k_{cat} of Trp570Tyr decreased 7.3-fold compared to that of the wild-type enzyme, while the K_m decreased 1.5-fold (Table 3). Trp570Phe retained 16.1 ± 1.0% of the WT activity; for the other substitutions, the activity was lower (Table 2). The k_{cat} of Trp570Phe decreased 4.5-fold, while the K_m increased 2.2-fold (Table 3). The kinetic parameters of Trp570Tyr and Trp570Phe show that the mutations at this site have a stronger influence on the turnover rate (k_{cat}) than on K_m and may affect acceptor binding. The GOS yields of the Trp570Tyr and Trp570Phe mutants were comparable with that of the WT enzyme (63.5 ± 0.8 g of GOS from 100 g of initial lactose), while Trp570Leu can produce only 43.8 ± 0.7 g of GOS from 100 g of initial lactose (Table 4). Mutants Trp570Tyr and Trp570Phe produced more of structure **8** and less of structures **11** and **17**, showing their preference for (β1→2) and (β1→3) over (β1→4) linkages. In contrast, Trp570Leu produced only 21.8 ± 0.5% of structure **8** compared to the wild type (100%), and the yield of structures further elongated from this (structure **13**) was too low to be quantified. The Trp570Leu yield of structure **11** was comparable to that of the wild-type enzyme. These results show the strong preference of this mutant to synthesize GOS with (β1→4) linkages. Notably, these three mutants also have a

DOI: 10.1021/acs.biochem.7b00207
Biochemistry 2017, 56, 3109−3118

Table 4. Total GOS Yields and Yields of the Major GOS Structures 8, 11, 13, and 17 Obtained for the *B. circulans* ATCC 31382 BgaD-D Trp570, Trp593, and Phe616 Mutants, Compared to the Wild-Type Enzyme[a]

enzyme	GOS yield[b]	structure **8** yield[c]	structure **11** yield[c]	structure **13** yield[c]	structure **17** yield[c]
WT[d]	63.5 ± 0.8	100	100	100	100
Trp570Tyr	65.8 ± 1.7	133.5 ± 0.9	52.7 ± 1.0	103.8 ± 1.6	41.3 ± 1.0
Trp570Phe	65.4 ± 0.9	110.1 ± 0.7	44.1 ± 0.5	91.6 ± 2.0	31.0 ± 0.6
Trp570Leu	43.8 ± 0.7	21.8 ± 0.5	93.9 ± 3.1	*e*	67.9 ± 2.7
Trp593Phe	66.0 ± 1.0	122.5 ± 5.1	65.7 ± 1.7	126.2 ± 5.1	53.7 ± 1.6
Trp593Tyr	65.2 ± 2.1	146.6 ± 7.2	49.3 ± 2.1	128.4 ± 1.9	35.4 ± 1.9
Phe616Trp	50.8 ± 2.4	80.8 ± 1.7	132.1 ± 7.2	75.7 ± 0.8	119.8 ± 6.0
Phe616Leu	61.0 ± 1.4	114.4 ± 1.6	91.3 ± 3.1	120.2 ± 2.5	82.7 ± 3.3
Phe616His	59.6 ± 1.2	99.8 ± 3.3	93.4 ± 1.5	110.6 ± 0.8	80.4 ± 2.4
Phe616Asn	57.3 ± 1.4	82.0 ± 2.6	106.5 ± 8.0	93.6 ± 4.7	97.3 ± 9.6
Phe616Tyr	58.3 ± 0.6	105.9 ± 4.3	108.0 ± 0.1	114.9 ± 2.0	108.3 ± 0.5

[a]GOS was produced using 3.75 units/mL β-galactosidase wild-type and mutant enzymes with 50% (w/w) lactose [in 100 mM sodium phosphate buffer (pH 6.0)] incubated at 60 °C for 20 h. [b]Yields are calculated as grams of GOS produced from 100 g of initial lactose. Calibration curves for lactose, galactose, and glucose ranging from 10 to 1000 μM were used for quantification. [c]The yields are relative to that of the wild-type enzyme (100%), estimated by comparing the peak intensities in the HPAEC−PAD profiles. [d]Data from our previous study.[11] [e]Unable to quantify.

Table 5. Total GOS Yields and Yields of the Major GOS Structures 8 and 11−13 Obtained for the *B. circulans* ATCC 31382 BgaD-D Asp481 and Lys487 Mutants, Compared to the Wild-Type Enzyme[a]

enzyme	GOS yield[b]	structure **8** yield[c]	structure **11** yield[c]	structure **12** yield[d]	structure **13** yield[c]
WT[e]	63.5 ± 0.8	100	100	0.2 ± 0.05	100
Asp481Glu	56.4 ± 2.2	51.5 ± 2.0	47.5 ± 1.5	4.8 ± 0.8	17.1 ± 3.2
Asp481Ser	55.3 ± 3.6	59.3 ± 1.9	70.1 ± 4.1	2.6 ± 0.4	30.3 ± 3.1
Asp481Asn	68.8 ± 1.7	68.5 ± 2.9	16.6 ± 0.8	4.9 ± 0.8	20.2 ± 4.7
Lys487Met	59.0 ± 1.9	99.8 ± 1.5	97.3 ± 3.2	*f*	103.2 ± 3.4
Lys487Phe	58.3 ± 1.5	74.7 ± 0.2	105.6 ± 1.3	1.6 ± 0.2	68.7 ± 1.0
Lys487Leu	59.1 ± 1.1	101.3 ± 0.7	101.9 ± 2.4	*f*	97.7 ± 4.1
Lys487Gln	58.6 ± 2.9	98.9 ± 1.2	98.8 ± 1.7	*f*	98.1 ± 2.9
Lys487Ser	63.6 ± 1.0	77.5 ± 3.1	68.2 ± 1.3	5.0 ± 0.4	57.5 ± 3.7
Lys487Gly	62.0 ± 2.7	63.1 ± 0.2	66.0 ± 2.7	9.7 ± 1.1	36.9 ± 3.7
Lys487Asn	59.8 ± 1.3	68.5 ± 1.8	104.4 ± 5.0	1.7 ± 0.2	58.5 ± 2.0

[a]GOS was produced using 3.75 units/mL β-galactosidase wild-type and mutant enzymes with 50% (w/w) lactose [in 100 mM sodium phosphate buffer (pH 6.0)] incubated at 60 °C for 20 h. [b]Yields are calculated as grams of GOS produced from 100 g of initial lactose. Calibration curves for lactose, galactose, and glucose ranging from 10 to 1000 μM were used for quantification. [c]The yields are relative to that of the wild-type enzyme (100%), estimated by comparing the peak intensities in the HPAEC−PAD profiles. [d]Yields are expressed as grams of product obtained from 100 g of initial lactose. A calibration curve of structure **12** [β-D-Gal*p*-(1→3)-β-D-Gal*p*-(1→4)-D-Glc*p*] ranging from 4 to 200 μg/mL was used for its quantification. [e]Data from our previous study.[11] [f]Not detectable.

higher hydrolytic activity, as evidenced by a much higher yield of galactose (structure **1**) compared to that of the wild-type enzyme (Figure 3A), i.e., 3.0, 5.9, and 10.1 times that of the wild type for Trp570Tyr, Trp570Phe, and Trp570Leu, respectively. Among the mutants of Trp593, activity was observed for only Trp593Tyr and Trp593Phe (3.3 ± 0.2 and 70.7 ± 0.7%, respectively) (Table 2). Both the K_m and the k_{cat} of Trp593Phe decreased (Table 3), resulting in a relatively low activity (70.7 ± 0.7%) compared to that of the wild-type enzyme (Table 2). As shown in panels B and F of Figure 3 and Table 4, the GOS yields of mutants Trp593Tyr and Trp593Phe were comparable to that of the wild-type enzyme. These two mutants synthesized more of structures **8** and **13** and less of structures **11** and **17**, showing their preference for (β1→2) and (β1→3) over (β1→4) linkages.

In the case of Phe616, the Phe616Tyr mutant had the highest activity, with 73.2 ± 0.6% of WT activity remaining, followed by Phe616Trp, which has 37.2 ± 1.5% of the WT activity (Table 2). The kinetic parameters (K_m and k_{cat}) of Phe616Tyr changed slightly compared to those of the wild-type enzyme (Table 3). For Phe616Trp, the K_m increased while the k_{cat} decreased (Table 3), resulting in a much lower activity. Phe616Trp produced more of structures **11** and **17** and less of structures **8** and **13** (Table 4), showing its preference for synthesizing (β1→4) linkages. In contrast, Phe616Leu has a preference for synthesizing (β1→2) and (β1→3) linkages (Figure 3C and Table 4).

The aromatic pocket formed by residues Trp570, Trp593, and Phe616 in BgaD shapes its active site. We found that mutations at these positions negatively affected enzyme activity, especially when the mutations were non-aromatic. Moreover, they changed the linkage preference and size of the products. For example, Trp570Leu produced only 21.8 ± 0.5% of structure **8** compared to the wild-type enzyme, and its elongation product, structure **13**, was not detectable. Apparently, the mutation enhanced the percentage of small oligosaccharides produced, achieving similar results as reported in a previous study.[37] Our results also show that Trp570 is essential for the transgalactosylation and hydrolysis activities, suggesting that it is involved in selection of the acceptor substrate, either water or carbohydrates. Together, the observed effects of mutations of residues in the aromatic pocket suggest that the geometry of this pocket is important to recognize and orient donor and acceptor substrates.

DOI: 10.1021/acs.biochem.7b00207
Biochemistry 2017, 56, 3109−3118

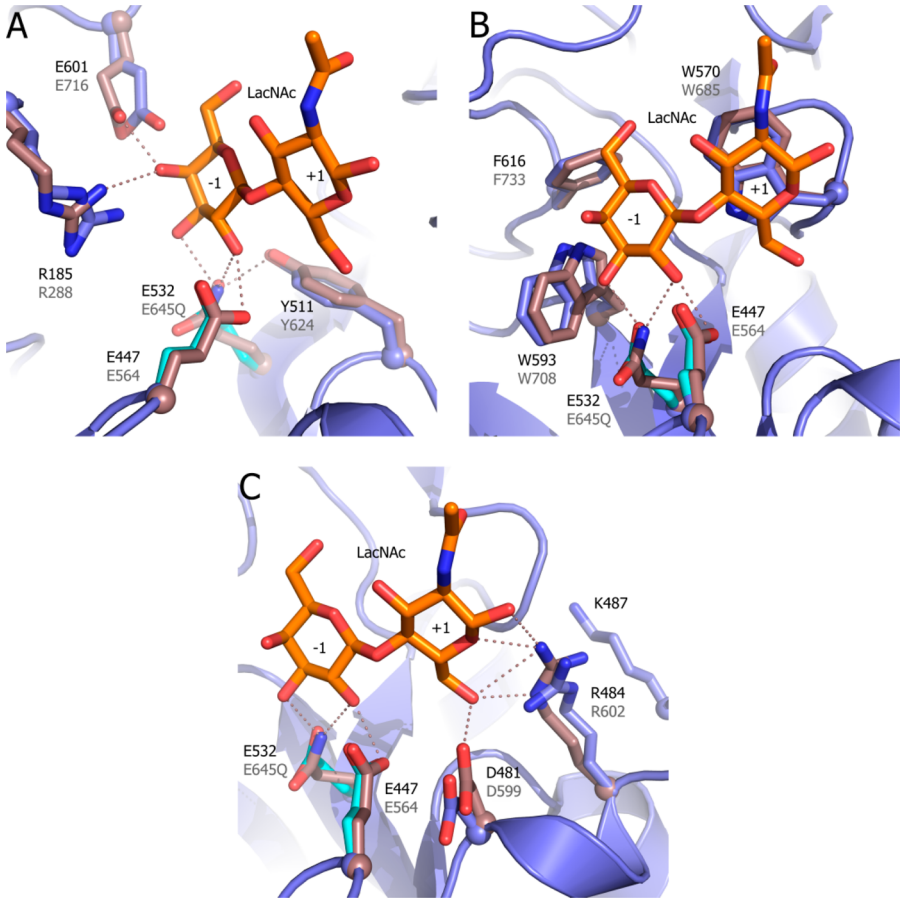

Figure 4. Superposition of the *B. circulans* ATCC 31382 BgaD-D residues (PDB code 4YPJ) subjected to mutagenesis [(A) Arg185, Glu601, and Tyr511, (B) Trp570, Trp593, and Phe616, and (C) Asp481 and Lys487] with the nucleophile mutant (E645Q) of BgaA of *S. pneumoniae* in complex with LacNAc (PDB code 4CUC). The color coding and labeling are the same as in Figure 2.

Asp481 and Lys487 Are Involved in Determining Linkage Specificity. Asp481, Arg484, and Lys487 are located near subsite +1 (Figure 4C). Mutations of the first residue (Asp481) dramatically reduced the enzyme activity. Among all mutants, only five (Glu, His, Ser, Asn, and Gln) retained some activity (Table 2). Because Asp481 is relatively close to the acid/base catalyst Glu447 (3.9 Å), mutations at this position may affect the orientation and/or acidity of Glu447 and thus influence catalysis. Mutation Asp481Gln increased the substrate binding affinity (K_m decreased 2-fold) but decreased the turnover rate (k_{cat} decreased 16-fold) (Table 3). The GOS profiles of the Asp481 mutants changed strongly compared to that of the wild-type enzyme (Figure 3D). The amounts of all major GOS structures produced by the wild-type enzyme (structures **8**, **11**, and **13**) decreased, while that of structure **12** increased significantly (Table 5), similar to results found previously for mutations of Arg484.[11] It is also notable that with mutant Asp481Asn, the yield of allolactose (structure **4**) increased 2.3-fold compared to that of the wild-type enzyme (Figure 3D). The results show that the mutations at this site favor synthesis of GOS with (β1→3) and (β1→6) linkages. In BgaA of *S. pneumoniae*, the corresponding Asp599 (Asp481 in BgaD) forms a hydrogen bond with the 6-OH group of the GlcNAc moiety at the +1 subsite (Figure 4C); thus, considering its position and interaction, Asp481 may play a role in acceptor substrate binding.

The third residue in this group, Lys487, is relatively far from the +1 subsite (Figure 4C). The activity of its mutants is relatively high compared to those of the other mutant enzymes except for Lys487Cys, retaining only 3.5 ± 0.4% of WT activity (Table 2). Compared to those of the wild-type enzyme, the K_m and k_{cat} values of Lys487Ser showed only minor changes. In comparison, the K_m value of Lys487Gly increased by 57% and resulted in a lower catalytic efficiency (k_{cat}/K_m = 1010). Compared with those of the wild-type enzyme, the GOS profiles and the relative amounts of the major structures did not change significantly for Lys487Met, Lys487Leu, or Lys487Gln. Mutants Lys487Phe, Lys487Ser, Lys487Gly, and Lys487Asn all have increased yields of structure **12** (Figure 3E and Table 5). Especially for Lys487Gly, the yield of structure **12** is comparable to that of Arg484Ser and Arg484His.[11] The latter mutations thus favor the synthesis of GOS with (β1→3) linkages. Considering the slightly larger distance from the +1 site, mutations of Lys487 may change the microenvironment of the +1 subsite, therefore affecting the linkage specificity indirectly.

CONCLUSIONS

In conclusion, we pinpointed several residues in the active site of BgaD that are important for the β-galactosidase reaction activity and specificity, by affecting substrate binding or transglycosylation specificity. Residues Arg185 and Glu601 at subsite −1 are essential for the β-galactosidase reaction because they affect substrate binding. A tyrosine residue near the catalytic residues (Tyr511) is also essential for the enzyme activity. An aromatic triplet (Trp570, Trp593, and Phe616) shaping the

DOI: 10.1021/acs.biochem.7b00207
Biochemistry 2017, 56, 3109−3118

active site is important for correct substrate binding and determining the linkage distribution. Residues in or near subsite +1 (Asp481, Asp484, and Lys487) may affect the acceptor substrate orientation. Mutants derived produced large amounts of the trisaccharide β-D-Galp-(1→3)-β-D-Galp-(1→4)-D-Glcp (structure **12**) in the product mixture, thus leading to more diverse GOS mixtures with potential industrial applications. Our study thus provides important insights into the understanding of the structure−function relationships of β-galactosidase enzymes, especially regarding their GOS product linkage specificity, and provides guidance for rational protein engineering of these enzymes with the aim of producing tailor-made prebiotic GOS mixtures.

■ ASSOCIATED CONTENT

Supporting Information

The Supporting Information is available free of charge on the ACS Publications website at DOI: 10.1021/acs.biochem.7b00207.

Primers used in this study and additional figures (PDF)

■ AUTHOR INFORMATION

Corresponding Author

*E-mail: L.Dijkhuizen@rug.nl.

ORCID

Huifang Yin: 0000-0001-8101-2430

Notes

The authors declare no competing financial interest.

■ ACKNOWLEDGMENTS

This work was funded by the China Scholarship Council (to H.Y.) and by the University of Groningen (to T.P., X.M., S.S.v.L., and L.D.). We also thank Prof. Johannis P. Kamerling for stimulating discussions.

■ REFERENCES

(1) Gibson, G. R., and Roberfroid, M. B. (1995) Dietary modulation of the human colonic microbiota: introducing the concept of prebiotics. *J. Nutr. 125*, 1401−1412.

(2) Gibson, G. R., Probert, H. M., Loo, J. V., Rastall, R. A., and Roberfroid, M. B. (2004) Dietary modulation of the human colonic microbiota: updating the concept of prebiotics. *Nutr. Res. Rev. 17*, 259−275.

(3) Bindels, L. B., Delzenne, N. M., Cani, P. D., and Walter, J. (2015) Towards a more comprehensive concept for prebiotics. *Nat. Rev. Gastroenterol. Hepatol. 12*, 303−310.

(4) Hutkins, R. W., Krumbeck, J. A., Bindels, L. B., Cani, P. D., Fahey, G., Goh, Y. J., Hamaker, B., Martens, E. C., Mills, D. A., Rastal, R. A., Vaughan, E., and Sanders, M. E. (2016) Prebiotics: Why definitions matter. *Curr. Opin. Biotechnol. 37*, 1−7.

(5) Coulier, L., Timmermans, J., Bas, R., Van Den Dool, R., Haaksman, I., Klarenbeek, B., Slaghek, T., and Van Dongen, W. (2009) In-depth characterization of prebiotic galacto-oligosaccharides by a combination of analytical techniques. *J. Agric. Food Chem. 57*, 8488−95.

(6) van Leeuwen, S. S., Kuipers, B. J. H., Dijkhuizen, L., and Kamerling, J. P. (2014) ^{1}H NMR analysis of the lactose/β-galactosidase-derived galacto-oligosaccharide components of Vivinal® GOS up to DP5. *Carbohydr. Res. 400*, 59−73.

(7) van Leeuwen, S. S., Kuipers, B. J. H., Dijkhuizen, L., and Kamerling, J. P. (2016) Corrigendum to "^{1}H NMR analysis of the lactose/β-galactosidase-derived galacto-oligosaccharide components of Vivinal® GOS up to DP5" [*Carbohydr. Res.* 400 (2014) 59−73]. *Carbohydr. Res. 419*, 69−70.

(8) Torres, D. P. M., Gonçalves, M. D. P. F., Teixeira, J. A., and Rodrigues, L. R. (2010) Galacto-oligosaccharides: Production, properties, applications, and significance as prebiotics. *Compr. Rev. Food Sci. Food Saf. 9*, 438−454.

(9) Bultema, J. B., Kuipers, B. J. H., and Dijkhuizen, L. (2014) Biochemical characterization of mutants in the active site residues of the β-galactosidase enzyme of *Bacillus circulans* ATCC 31382. *FEBS Open Bio 4*, 1015−20.

(10) Yin, H., Bultema, J. B., Dijkhuizen, L., and van Leeuwen, S. S. (2017) Reaction kinetics and galactooligosaccharide product profiles of the β-galactosidases from *Bacillus circulans*, *Kluyveromyces lactis* and *Aspergillus oryzae*. *Food Chem. 225*, 230−238.

(11) Yin, H., Pijning, T., Meng, X., Dijkhuizen, L., and van Leeuwen, S. S. (2017) Engineering of the *Bacillus circulans* β-galactosidase product specificity. *Biochemistry 56*, 704−711.

(12) Cantarel, B. L., Coutinho, P. M., Rancurel, C., Bernard, T., Lombard, V., and Henrissat, B. (2009) The Carbohydrate-Active EnZymes database (CAZy): An expert resource for glycogenomics. *Nucleic Acids Res. 37*, D233−D238.

(13) Gosling, A., Stevens, G. W., Barber, A. R., Kentish, S. E., and Gras, S. L. (2010) Recent advances refining galactooligosaccharide production from lactose. *Food Chem. 121*, 307−318.

(14) Husain, Q. (2010) β-Galactosidases and their potential applications: a review. *Crit. Rev. Biotechnol. 30*, 41−62.

(15) Otieno, D. O. (2010) Synthesis of β-galactooligosaccharides from lactose using microbial β-galactosidases. *Compr. Rev. Food Sci. Food Saf. 9*, 471−482.

(16) Nakanishi, K., Matsuno, R., Torii, K., Yamamoto, K., and Kamikubo, T. (1983) Properties of immobilized β-D-galactosidase from *Bacillus circulans*. *Enzyme Microb. Technol. 5*, 115−120.

(17) Usui, T., Kubota, S., and Ohi, H. (1993) A convenient synthesis of β-D-galactosyl disaccharide derivatives using the β-D-galactosidase from *Bacillus circulans*. *Carbohydr. Res. 244*, 315−323.

(18) Yanahira, S., Kobayashi, T., Suguri, T., Nakakoshi, M., Miura, S., Ishikawa, H., and Nakajima, I. (1995) Formation of oligosaccharides from lactose by *Bacillus circulans* β-galactosidase. *Biosci., Biotechnol., Biochem. 59*, 1021−1026.

(19) Song, J., Abe, K., Imanaka, H., Imamura, K., Minoda, M., Yamaguchi, S., and Nakanishi, K. (2011) Causes of the production of multiple forms of β-galactosidase by *Bacillus circulans*. *Biosci., Biotechnol., Biochem. 75*, 268−278.

(20) Vetere, A., and Paoletti, S. (1998) Separation and characterization of three β-galactosidases from *Bacillus circulans*. *Biochim. Biophys. Acta, Gen. Subj. 1380*, 223−231.

(21) Song, J., Imanaka, H., Imamura, K., Minoda, M., Katase, T., Hoshi, Y., Yamaguchi, S., and Nakanishi, K. (2011) Cloning and expression of a β-galactosidase gene of *Bacillus circulans*. *Biosci., Biotechnol., Biochem. 75*, 1194−1197.

(22) Warmerdam, A., Paudel, E., Jia, W., Boom, R. M., and Janssen, A. E. M. (2013) Characterization of β-galactosidase isoforms from *Bacillus circulans* and their contribution to GOS production. *Appl. Biochem. Biotechnol. 170*, 340−58.

(23) Song, J., Imanaka, H., Imamura, K., Minoda, M., Yamaguchi, S., and Nakanishi, K. (2013) The discoidin domain of *Bacillus circulans* β-galactosidase plays an essential role in repressing galactooligosaccharide production. *Biosci., Biotechnol., Biochem. 77*, 73−79.

(24) Ishikawa, K., Kataoka, M., Yanamoto, T., Nakabayashi, M., Watanabe, M., Ishihara, S., and Yamaguchi, S. (2015) Crystal structure of β-galactosidase from *Bacillus circulans* ATCC 31382 (BgaD) and the construction of the thermophilic mutants. *FEBS J. 282*, 2540−2552.

(25) Boehm, G., Fanaro, S., Jelinek, J., Stahl, B., and Marini, A. (2003) Prebiotic concept for infant nutrition. *Acta Paediatr. 92*, 64−67.

(26) Osborn, D. A., and Sinn, J. K. H. (2007) Probiotics in infants for prevention of allergic disease and food hypersensitivity. *Cochrane Database of Systematic Reviews*, 1−3.

(27) Knol, J., Scholtens, P., Kafka, C., Steenbakkers, J., Groβ, S., Helm, K., Klarczyk, M., Schöpfer, H., Böckler, H.-M., and Wells, J. (2005) Colon microflora in infants fed formula with galacto- and

DOI: 10.1021/acs.biochem.7b00207
Biochemistry 2017, 56, 3109−3118

fructo-oligosaccharides: more like breast-fed infants. *J. Pediatr. Gastroenterol. Nutr. 40*, 36−42.
(28) Fanaro, S., Boehm, G., Garssen, J., Knol, J., Mosca, F., Stahl, B., and Vigi, V. (2005) Galacto-oligosaccharides and long-chain fructo-oligosaccharides as prebiotics in infant formulas: a review. *Acta Paediatr. 94*, 22−26.
(29) Whisner, C. M., Martin, B. R., Schoterman, M. H. C., Nakatsu, C. H., McCabe, L. D., McCabe, G. P., Wastney, M. E., van den Heuvel, E. G. H. M., and Weaver, C. M. (2013) Galacto-oligosaccharides increase calcium absorption and gut bifidobacteria in young girls: a double-blind cross-over trial. *Br. J. Nutr. 110*, 1292−1303.
(30) Monteagudo-Mera, A., Arthur, J. C., Jobin, C., Keku, T., Bruno-Barcena, J. M., and Azcarate-Peril, M. A. (2016) High purity galacto-oligosaccharides enhance specific *Bifidobacterium* species and their metabolic activity in the mouse gut microbiome. *Benefic. Microbes 7*, 247−264.
(31) Bruno-Barcena, J. M., and Azcarate-Peril, M. A. (2015) Galacto-oligosaccharides and colorectal cancer: Feeding our intestinal probiome. *J. Funct. Foods 12*, 92−108.
(32) Lamsal, B. P. (2012) Production, health aspects and potential food uses of dairy prebiotic galactooligosaccharides. *J. Sci. Food Agric. 92*, 2020−2028.
(33) Juers, D. H., Matthews, B. W., and Huber, R. E. (2012) LacZ β-galactosidase: structure and function of an enzyme of historical and molecular biological importance. *Protein Sci. 21*, 1792−1807.
(34) Pereira-Rodríguez, A., Fernández-Leiro, R., González-Siso, M. I., Cerdán, M. E., Becerra, M., and Sanz-Aparicio, J. (2012) Structural basis of specificity in tetrameric *Kluyveromyces lactis* β-galactosidase. *J. Struct. Biol. 177*, 392−401.
(35) Skálová, T., Dohnálek, J., Spiwok, V., Lipovová, P., Vondráčková, E., Petroková, H., Dušková, J., Strnad, H., Králová, B., and Hašek, J. (2005) Cold-active β-galactosidase from *Arthrobacter* sp. C2−2 forms compact 660 kDa hexamers: crystal structure at 1.9A resolution. *J. Mol. Biol. 353*, 282−94.
(36) Rutkiewicz-Krotewicz, M., Pietrzyk-Brzezinska, A. J., Sekula, B., Cieśliński, H., Wierzbicka-Woś, A., Kur, J., and Bujacz, A. (2016) Structural studies of a cold-adapted dimeric β-D-galactosidase from *Paracoccus* sp. 32d. *Acta Crystallogr. Sect. D, Struct. Biol. 72*, 1049−61.
(37) Tanaka, S., Takahashi, T., Koide, A., Ishihara, S., Koikeda, S., and Koide, S. (2015) Monobody-mediated alteration of enzyme specificity. *Nat. Chem. Biol. 11*, 762−764.

DOI: 10.1021/acs.biochem.7b00207
Biochemistry 2017, 56, 3109−3118